Available online at www.sciencedirect.com

SCIENCE DIRECT®

Geomorphology 63 (2004) 131–143

GEOMORPHOLOGY

www.elsevier.com/locate/geomorph

Rainfall thresholds for landsliding in the Himalayas of Nepal

Emmanuel J. Gabet[a,*], Douglas W. Burbank[a,1], Jaakko K. Putkonen[b,2], Beth A. Pratt-Sitaula[a,3], Tank Ojha[c]

[a] *Department of Geological Sciences, University of California, Santa Barbara, CA 93110, USA*
[b] *Quaternary Research Center and Department of Earth and Space Sciences, University of Washington, Seattle, WA 98195, USA*
[c] *Himalayan Experience, Kathmandu, Nepal*

Received 12 August 2003; received in revised form 23 March 2004; accepted 31 March 2004
Available online 19 June 2004

Abstract

Landsliding of the hillslope regolith is an important source of sediment to the fluvial network in the unglaciated portions of the Himalayas of Nepal. These landslides can produce abrupt increases of up to three orders of magnitude in the fluvial sediment load in less than a day. An analysis of 3 years of daily sediment load and daily rainfall data defines a relationship between monsoonal rainfall and the triggering of landslides in the Annapurna region of Nepal. Two distinct rainfall thresholds, a seasonal accumulation and a daily total, must be overcome before landslides are initiated. To explore the geomorphological controls on these thresholds, we develop a slope stability model, driven by daily rainfall data, which accounts for changes in regolith moisture. The pattern of rainfall thresholds predicted by the model is similar to the field data, including the decrease in the daily rainfall threshold as the seasonal rainfall accumulation increases. Results from the model suggest that, for a given hillslope, regolith thickness determines the seasonal rainfall necessary for failure, whereas slope angle controls the daily rainfall required for failure.

Keywords: landslides; Himalayas; climatic thresholds; Nepal

1. Introduction

The steep slopes, weathered bedrock, and intense monsoonal rainfall of the Nepalese Himalayas create ideal conditions for landslides. Analyses and case studies of hillslope failures by Shroder (1998) and Shroder and Bishop (1998) have shown that landslides are the primary agent of hillslope erosion in the unglaciated regions of the Himalayas. During the monsoon seasons of 2000–2002, we measured suspended sediment concentrations and discharge in a catchment in the High Himalayas of Nepal; and with

* Corresponding author. Present address: Department of Geology, University of Montana, Missoula, MT 59812, USA. Tel.: +1-406-243-4761; fax: +1-406-243-4028.
E-mail addresses: manny.gabet@mso.umt.edu (E.J. Gabet), burbank@crustal.ucsb.edu (D.W. Burbank), putkonen@u.washington.edu (J.K. Putkonen), pratt@crustal.ucsb.edu (B.A. Pratt-Sitaula).
[1] Tel.: +1-805-893-7858; fax: +1-805-893-2314.
[2] Tel.: +1-206-543-0689; fax: +1-206-543-0489.
[3] Tel.: +1-805-893-7242; fax: +1-805-893-2314.

0169-555X/$ - see front matter © 2004 Elsevier B.V. All rights reserved.
doi:10.1016/j.geomorph.2004.03.011

these measurements, we calculated daily suspended sediment load. Although sediment loads were typically low (<700 tons/day), they were intermittently punctuated by loads that were up to three orders of magnitude greater than background rates (Fig. 1). The source of this suspended sediment appears linked to landslides triggered by rainfall. The pulsatory nature of the sediment loading is consistent with sediment delivery from landslides (e.g., Hovius et al., 2000); and landslide scars, as seen from field observations and aerial photographs, are ubiquitous throughout the watershed. The poor relationship between high flows and high sediment loads is evidence that the channels are supply-limited and dependent on inputs of sediment from the hillslopes. For example, the three peak discharges in July and August 2001 are not matched by equivalent peaks in sediment load (Fig. 1). Finally, negligible amounts of sediment stored in the valleys and channels further support our conclusion that landslides are the source of the sediment pulses.

Several studies have attempted to define rainfall thresholds for the triggering of landslides. Some have used empirical intensity-duration thresholds (Caine, 1980; Caine and Mool, 1982; Cannon and Ellen, 1985; Larsen and Simon, 1993), whereas others have proposed more process-based approaches (Keefer et al., 1987; Crozier, 1999). The simple intensity-duration models may be robust for a particular region, but they provide a minimal amount of insight into the actual physical processes that trigger landslides. In contrast, Crozier's (1999) soil-moisture model of landslide initiation incorporates hydrological processes such as evapotranspiration and the drainage of soil-water. In this study, we couple Crozier's (1999) soil-moisture model to a slope stability analysis and apply them to our field area. The motivation for this study was threefold. First, the identification of rainfall amounts that lead to landslides may help mitigate the loss of life and property in the many Nepalese communities clinging to the steep Himalayan hillsides. Second, developing a quantitative model relating rainfall to landslide initiation may provide insight into the process of landslide initiation in the Himalayas and similar areas. Finally, exploring how rainstorms trigger landslides is critical in understanding the linkages between orogenic and climatic processes.

2. Materials and methods

2.1. Site description

The Khudi Khola (Khola = River) drains a 136-km^2 catchment on the southern flank of the Anna-

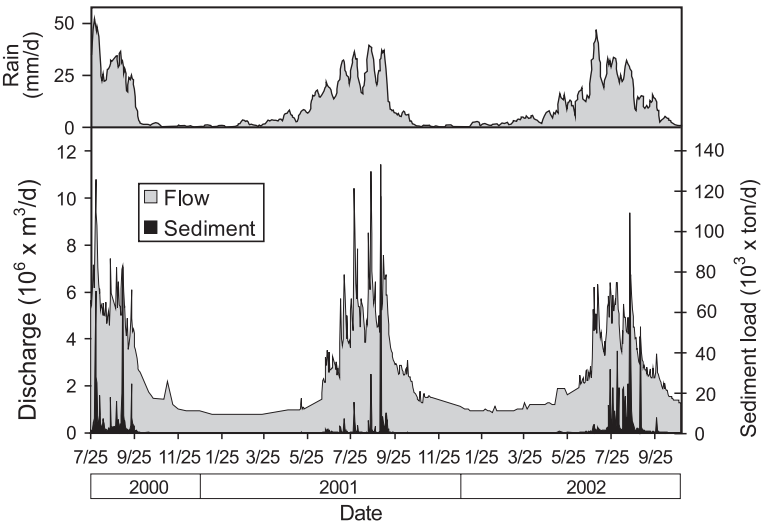

Fig. 1. River discharge, sediment load, and rainfall data from the Khudi catchment. Rainfall data are smoothed by averaging over a 10-day moving window. Note that the sediment load measurements did not begin until the monsoon had already begun in 2000.

purna Himalayas (Fig. 2). The mean elevation of the catchment is 2565 m (Fig. 3A), and the bedrock consists of schists and gneisses (Colchen et al., 1986). The catchment receives heavy seasonal orographic rainfall (3000–5000 mm/year) as monsoon-driven moisture impinges upon the southern flank of the Annapurna range to yield an average annual rainfall of ~4000 mm. High rock-uplift rates (~2 mm/year; Burbank et al., 2003) coupled with the heavy rainfall produce rugged topography with steep slopes and high relief. The mean hillslope angle, measured from a 3-arc-second digital elevation model (DEM) is $26 \pm 8°$ (1σ) (Fig. 2B). Although average soil depths are only about 0.50 m, the underlying bedrock is also deeply weathered and permeable (J. Garcia, Harvard University, personal communication, 2003). The hydrologically active portion of the hillslope mantle (soil and weathered bedrock) will be subsequently referred to as the regolith.

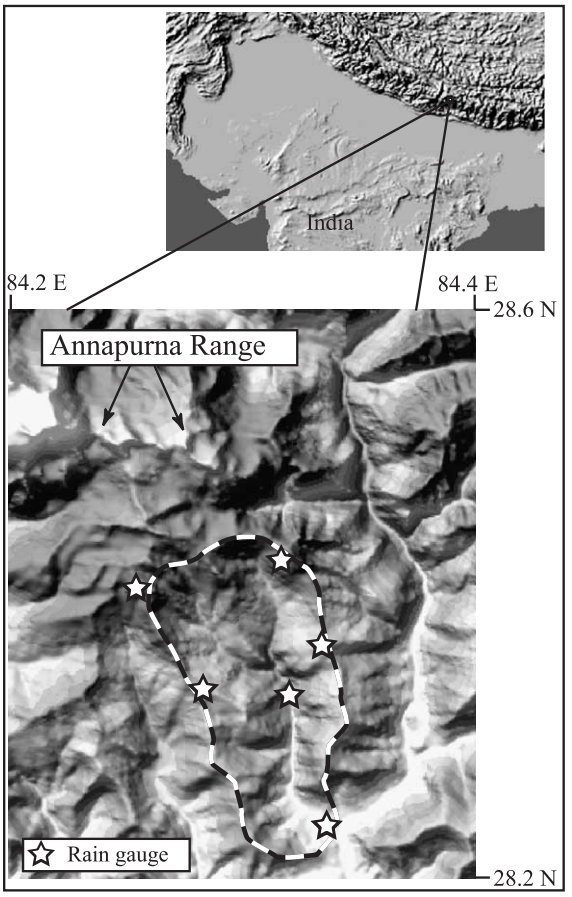

Fig. 2. Maps of region and study site. Stars indicate locations of meteorological stations used in this study.

2.2. Data collection

In 1999, a network of automated rain gauges was installed throughout the Khudi catchment (Barros et al., 2000). On the basis of data quality, record length, and areal coverage, half-hour rainfall data from six of the loggers were summed to calculate areally weighted daily rainfall values for the entire catchment.

During three monsoon seasons spanning 2000–2002, three 500-cm^3 surface water samples were collected twice daily from the Khudi Khola at a surveyed cross-section. These samples were filtered, the dried sediment was weighed, and the mass of the sediment from the three samples was averaged to calculate an average sediment concentration. The discharge at the cross section (mean monsoonal discharge = 45 m^3/s) was determined by multiplying the flow velocity, estimated with the floating-boat method (Leopold et al., 1964), with the cross-sectional area of the flow. Sediment load was simply calculated as the product of sediment concentration and discharge. Because the bed load constitutes an unknown fraction of the total load, we were measuring a minimum sediment load.

2.3. Determination of rainfall thresholds

We only considered daily sediment loads >2310 tons; such loads constituted 90% of the entire measured sediment load during the 2000–2002 monsoons. From the daily loads >2310 tons, we defined sediment peaks as increases in sediment load greater than the previous day's load; and we assumed that these sediment peaks were due to an input of landslide debris into the fluvial network. Over the 3-year record, 48 sediment peaks met the daily sediment load criterion and were used to determine landslide-triggering thresholds.

The 48 sediment peaks were used to determine values for three different rainfall thresholds. The first threshold, determined daily, is the total rainfall since the beginning of the monsoon season. The second threshold is a "moving window" total that is the total rainfall recorded over the past x days. An optimiza-

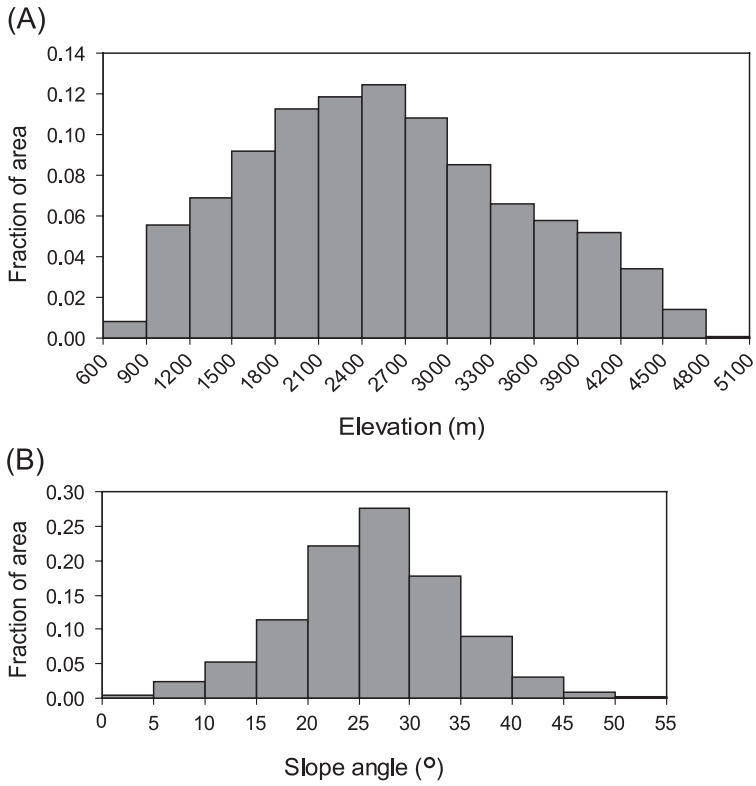

Fig. 3. (A) Distribution of elevation in the Khudi catchment determined from the 90-m DEM. (B) Distribution of slope angles in the Khudi catchment determined from the 90-m DEM.

tion algorithm was used to determine the best-fit value for the length of the moving window threshold. The third threshold is the daily rainfall total. Because we were unable to determine the source of the sediment, the three thresholds were applied to rainfall amounts averaged over the entire Khudi catchment. Although we did not account for the effect of human disturbance on landslide thresholds, Marston et al. (1998) concluded that human activity does not generally affect landslide frequency in the Himalayas of central Nepal.

Inherent in our analysis is the assumption that the suspended sediment travels down the catchment rapidly enough that the rainfall data and the suspended sediment data are temporally coincident. Data from monitoring stations along the length of a nearby river indicate that suspended sediment waves commonly travel 2–3 m/s. Because the Khudi catchment is 18 km long, a sediment peak could travel from the farthest point to the outlet in <3 h.

3. Results and discussion

3.1. Thresholds

We found that landslides are not triggered until ~ 860 mm of rain have fallen during the monsoon (Fig. 4). These observations suggest that sufficient antecedent rainfall is necessary to bring the regolith up to field capacity (the soil moisture beyond which gravity drainage will ensue) such that future rainfall may produce positive pore pressures and trigger landslides (Campbell, 1975; Crozier, 1999). A decrease in the ratio of rainfall to runoff during the early monsoon season supports the hypothesis that a portion of rainwater from the first storms is stored in the regolith (Fig. 5). Once field capacity is reached, the ratio of rainfall to runoff remains approximately constant throughout the remainder of the primary monsoon season. Similar to this seasonal threshold, Larsen and Simon (1993) noted that landslides in

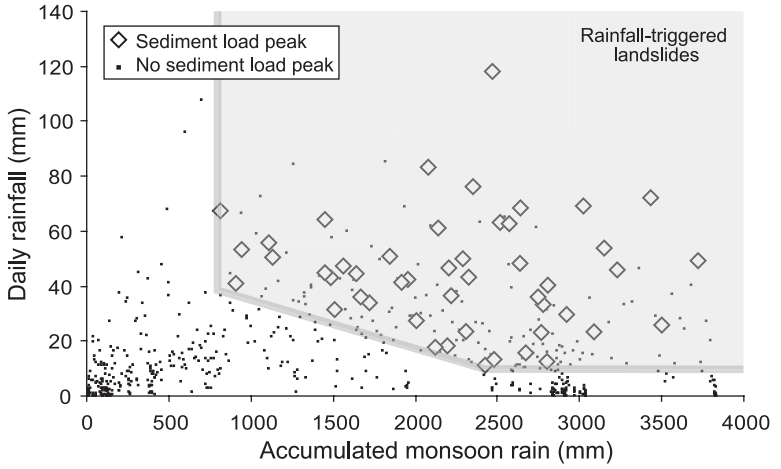

Fig. 4. Rainfall thresholds for sediment peaks. The shaded area delineates the rainfall values that may trigger landslides (shown by diamonds). Note that there are no failures until a total of 860 mm of rain had fallen and that the daily rainfall threshold decreased with increasing accumulated rainfall until it reached a minimum of 11 mm. Accumulated rainfall is a rough proxy for time.

Puerto Rico tended to cluster near the end of the hurricane season, Matthias and Weatherly (2003) found that landslide initiation in British Columbia was dependent on the prior 4 weeks of rainfall, and Wieczorek (1987) observed that debris flows that began as landslides in a region of California did not occur until 280 mm of rainfall had fallen during the wet season.

Surprisingly, the inclusion of a moving window threshold was not warranted, regardless of window length. This result contrasts with that by Chleborad (2000) in which a 3-day antecedent rainfall total was found to be a useful threshold for predicting landslide initiation near Seattle, WA. The lack of a window threshold for landslides in the Khudi catchment suggests that the regolith attains field capacity and remains there. A window threshold would only be relevant if sufficient time elapsed between storms that regolith moistures dropped significantly below field capacity. The nearly daily rain of the monsoon

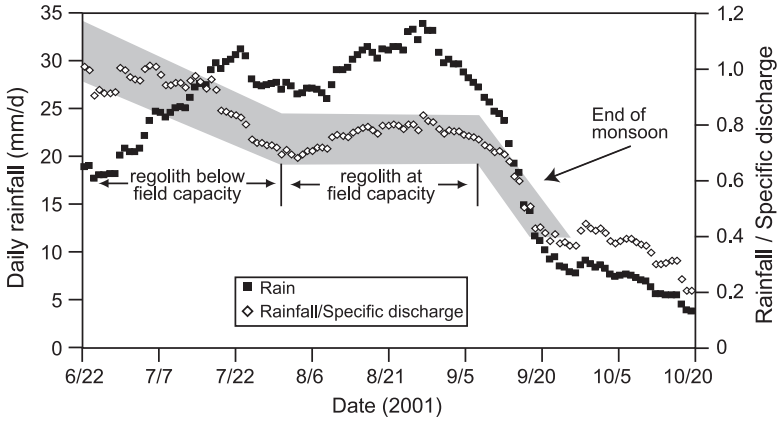

Fig. 5. Decrease in the ratio of observed rainfall to specific discharge (averaged over a 20-day window) in the early stages of the 2001 monsoon (6/22-7/22) indicates that a progressively smaller portion of rainfall is stored in the regolith. The ratio becomes approximately constant from 7/22 until the end of the monsoon, suggesting that the regolith has generally attained field capacity at this point.

season rarely allows the regolith to dry much below field capacity.

The daily rainfall threshold appears to decrease with increasing seasonal accumulation, reaching a minimum and becoming constant at ~ 11 mm/day (Fig. 4). Similarly, Crozier's (1999) data indicated that progressively smaller daily rainfall amounts are needed to trigger landslides as soil moisture increases. We interpret the initial decline of the daily rainfall threshold to be a function of the distribution of slope angles and regolith depths throughout the watershed. In general, we predict that thinner regolith on steeper slopes will fail sooner than will thicker regolith on gentler slopes. We explore the relationships between rainfall, hillslope characteristics, and slope failures with a numerical model.

3.2. Model

When the 48 sediment peaks are considered in the context of the rainfall record (Fig. 4), a discrete field of landslide susceptibility becomes readily apparent. A key goal of this study is to develop a process-based model that explains the controls on the boundaries of the landsliding field. Our numerical model applies a hillslope-stability analysis, coupled to a regolith-moisture model, to the Khudi catchment. In this model, the regolith-bedrock contact provides both a hydrological boundary as well as the basal slip surface for landsliding. In an approach similar to Benda and Dunne (1997) and Gabet and Dunne (2003), we populated the model space with a distribution of hillslopes ($n = 13{,}340$) and each hillslope is assigned a hillslope angle and regolith thickness randomly drawn from probability distributions. The distribution of hillslope angles was determined from a 3-arcsecond (~ 90-m grid spacing) DEM of the Khudi catchment (Fig. 3B). Although hillslope lengths at the study site may exceed the window size used to calculate slope angles (~ 270 m), we assumed that the measured slope distribution approximates the distribution of hillslope angles. On the basis of our limited field observations of landslide depths and data from another study (Caine and Mool, 1982), we assumed that regolith thickness is normally distributed with a mean of 4 ± 1.5 m (1σ). Although this approach may combine a very steep hillslope angle with a thick regolith, all unconditionally unstable hillslopes (i.e., hillslopes that fail without positive pore pressures) are removed before the start of the model runs.

A regolith-moisture index and water-table height are determined for each hillslope according to Crozier's (1999) hillslope hydrology model (modified to account for the interception of rainfall by vegetation). The inputs, outputs, and storage of water in the model (Fig. 6) are governed by two basic rules: (i) positive pore pressures, necessary for triggering landslides, do not develop until the moisture exceeds the regolith's field capacity (Campbell, 1975; Crozier, 1999); and (ii) moisture in excess of field capacity is rapidly drained (Crozier, 1999).

The initial value of the moisture index (M_0; mm) is taken to be the negative of the field capacity (F_c; mm) such that, at the end of the dry season,

$$M_0 = -F_c \tag{1a}$$

where

$$F_c = H(n - n_d), \tag{1b}$$

n is total porosity, n_d is drained porosity, and H is regolith thickness (mm) measured vertically. The

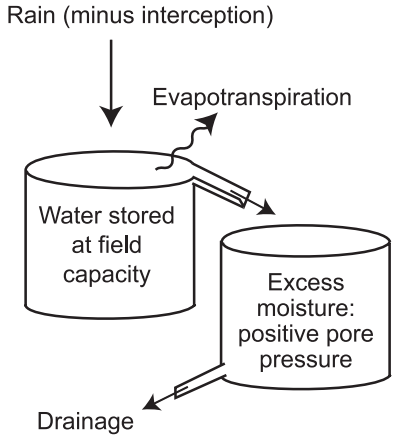

Fig. 6. The regolith-moisture model. Rainfall that is not intercepted by vegetation infiltrates into the regolith. This water is initially stored within the regolith and a fraction of it is lost to evapotranspiration. When field capacity is reached, additional inputs of rain contribute to the excess moisture and create positive pore pressures. The excess moisture, however, is rapidly drained.

effective rainfall at time t that contributes water to the hillslope, R_t (mm), is determined with

$$R_t = P_t - I \tag{2}$$

where P_t is total daily rainfall (mm) at time t and I is the amount of rain (mm) intercepted by vegetation. Daily moisture values are calculated with

$$M_t = M_{t-1} + R_t - D_t - E_t \tag{3}$$

where M_{t-1} is the previous day's value of the moisture index and E_t is the daily evapotranspiration (mm). The drainage term in Eq. (3), D_t (mm), is determined as

$$D_t = \begin{cases} 0 & \text{if } M_{t-1} \leq 0 \\ kM_{t-1} & \text{if } M_{t-1} > 0 \end{cases} \tag{4}$$

where k is a dimensionless constant. D_t accounts for water that drains quickly from the regolith after the field capacity has been exceeded. An illustration of the temporal evolution of a hillslope's moisture index during the monsoon is shown in Fig. 7. Finally, the height of the water table, h (m), above the regolith-bedrock contact, measured normal to the hillslope surface, is calculated from positive values of M_t with

$$h = 10^{-3} M_t n_{\mathrm{d}} \tag{5}$$

where M_t is converted from mm to m.

This moisture model is coarse and not entirely physically based. For example, the drainage term grossly simplifies the process of subsurface flow and does not account for the effect of hillslope angle. Additionally, the effect of bedrock topography on subsurface flow convergence, an important factor in slope failure (Anderson and Burt, 1978), is ignored; and the soil and highly weathered bedrock are assumed to have similar hydrologic properties. Nonetheless, we suggest that this model captures the essence, if not the details, of hillslope hydrology.

Because field observations indicate that the majority of the landslides in the region have failure planes approximately parallel to the slope surface, we use Iverson's (2000) infinite slope stability analysis to

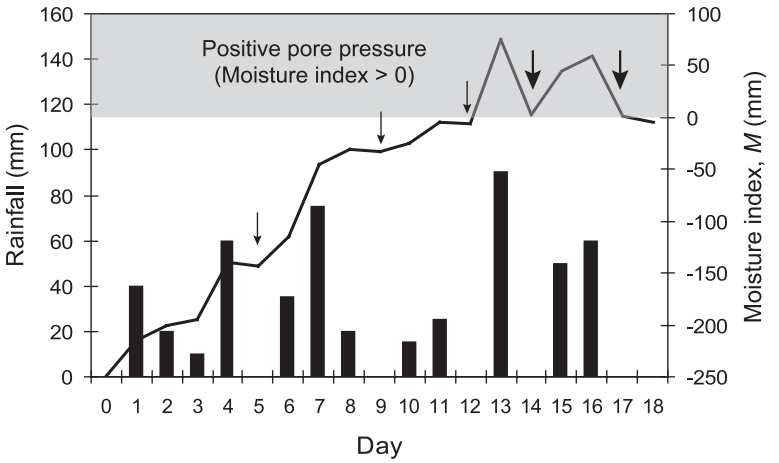

Fig. 7. Hypothetical example of changes in the moisture index according to the model. Columns represent daily rainfall and the line represents moisture index (M). Positive pore pressures (represented by gray area) develop when the moisture index exceeds the field capacity. Small arrows indicate soil moisture decreases due to evapotranspiration and large arrows indicate soil moisture decreases due to evapotranspiration and drainage. Note that excess moisture is rapidly drained between storms once the field capacity is reached. Interception = 2 mm/day, evapotranspiration = 5 mm/day, $k = 0.9$, field capacity = 250 mm.

determine which hillslopes fail. The pressure head, ψ_t (m), at time t is determined with

$$\psi_t = h\cos\theta \tag{6}$$

The pressure head, calculated daily for each hillslope, is applied to

$$F_s = \frac{\tan\phi}{\tan\theta} + \frac{C - \psi_t \gamma_w \tan\phi}{\gamma_r H \sin\theta\cos\theta} \tag{7}$$

which predicts a slope failure when the factor-of-safety, F_s, drops below unity (Iverson, 2000). ϕ is the internal angle of friction (deg), C is cohesion (Pa), γ_w is the unit weight of water (N/m^3), and γ_r is the unit weight of the regolith. Note that we are assuming that the role of root strength is negligible, even though these hillslopes are highly vegetated. Marston et al. (1998) found somewhat mixed evidence regarding deforestation and landslide frequency, suggesting that plant roots may not have a dominant role in preventing landslides. In general, it is a given that plant roots help to stabilize soil against landsliding but it is not clear whether the roots on the Himalayan slopes are deep enough to have a significant effect. Furthermore, high rainfall rates and warm temperatures that lead to rapid litter decay may yield an ample supply of water and nutrients at the soil surface, possibly obviating the need for deep roots (Usman et al., 1999; Schenk and Jackson, 2002). Therefore, given all the uncertainties in the other terms involved in our model, we feel that the error in assuming a negligible contribution of root strength is small.

Values for the hydrological and geotechnical parameters (Table 1) were drawn from various sources that are unlikely to duplicate precisely the conditions in the Khudi catchment but are reasonable. In the model, evapotranspiration values change temporally according to results presented by Lambert and Chitrakar (1989), such that values are at a maximum of 3.5 mm/day at the beginning of the monsoon and decrease to 2.3 mm/day by the monsoon's end. Values for total porosity and drainable porosity are rough estimates. Errors in these two variables will affect the calculated storage capacity of the regoliths but not the pattern of the results.

Table 1
Parameter values for model

Variable	Value	Source
C	4000 Pa	Caine and Mool, 1982
I	1 mm/day	Lloyd et al., 1988
k	0.9	Dunne and Leopold, 1978
n	0.40	estimated
n_d	0.15	estimated
E_t	2.3–3.5 mm/day	Lambert and Chitrakar, 1989[a]
γ_s	19,620 N/m^3	estimated
γ_w	9810 N/m^3	
ϕ	37°	Caine and Mool, 1982

[a] The authors calculated values for potential evapotranspiration that we assumed to be equal to actual evapotranspiration during the monsoon. The values shown here represent the range during the monsoon season.

The 3-year rainfall record from one of the automated rain gauges was used as the rainfall input for the model, and the model was run at a daily time-step. Results from the model (Fig. 8A) show a pattern of thresholds similar to the field data (Fig. 4). An important caveat, however, to comparisons between the model results and the field data is that the rainfall values for the field data are averages for the entire catchment. This averaging may bias the observed thresholds toward lower values because the landslides are likely occurring in parts of the catchment where the rainfall is the most intense.

The model predicts that a minimum seasonal rainfall (528 mm) must accumulate and a minimum daily rainfall (9 mm) must be exceeded before landslides are triggered (Fig. 8A). In the model, the position of the thresholds is sensitive to different controlling variables (Fig. 8B). Because landslides do not occur until the field capacity is exceeded, a certain amount of rain must fall to initially wet the regolith; and thus, the seasonal accumulation threshold is a function of the regolith thickness and porosity (both total and drained). The daily precipitation threshold is due, in part, to evapotranspiration and interception losses that must be overcome before any rainfall can contribute to the regolith's moisture. These losses amount to less than half of the daily precipitation threshold; the balance represents a minimum positive pore pressure needed to produce a failure.

Whereas the modeled daily threshold is nearly identical to the field observations, the seasonal thresh-

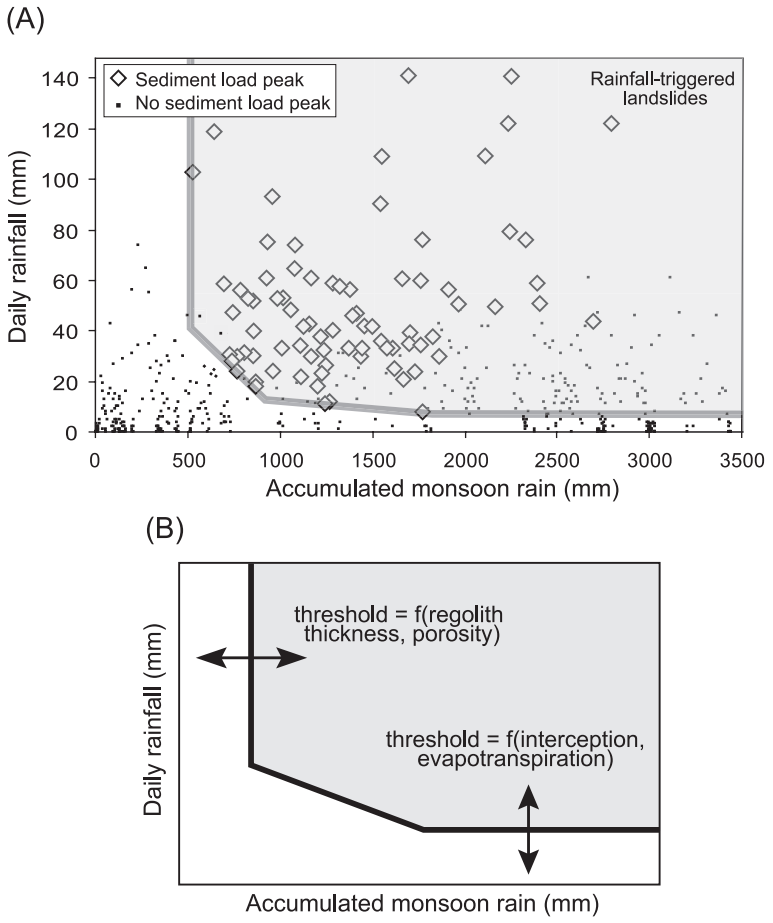

Fig. 8. (A) Results from the coupled regolith moisture and hillslope stability analysis model. Although the predicted seasonal accumulation threshold is less than that observed from the field data (compare with Fig. 4), the general pattern of thresholds is similar. Note the declining daily rainfall threshold as the monsoon season progresses. (B) The field capacity, determined as a function of regolith thickness and porosity, controls the seasonal accumulation threshold because failures will not occur until the field capacity is exceeded. Rainfall interception and evapotranspiration provide important controls on the daily precipitation threshold. Rainfall must exceed these losses before positive pore pressures can develop in the regolith. The diagonal threshold between the seasonal accumulation and daily precipitation thresholds is a function of the distribution of regolith thicknesses and slope angles.

old is substantially lower. This may be because, in the model, water does not drain from the regolith until the field capacity is exceeded. In reality, an unknown percentage of the subsurface water may be lost through macropore flow, even before the regolith becomes saturated (Beven and Germann, 1982). Significant amounts of water flowing into the bedrock would also account for the discrepancy. Finally, underestimations of the regolith thickness or porosity might explain the lower modeled seasonal threshold. There is evidence, however, that the estimates of regolith thickness and porosity may be approximately correct. The total volume of rain (minus interception and evapotranspiration) falling on the basin up until the time when the regolith attains field capacity (Fig. 5) is 1.87×10^8 m^3. Assuming that the total volume of discharge (1.25×10^8 m^3) in the Khudi Khola, during the same time period, is direct runoff from the rainfall, then the depth of water stored in the regolith at field capacity is 0.46 m. Taking the other endmember where flow in the Khudi Khola is entirely from baseflow with no contributions from that season's

rainfall, the depth of water stored at field capacity is 1.37 m. Eq. (1b), solved with the values used in the model (Table 1) yields an average field capacity of 1 m. The endmember field capacities estimated from the rainfall and flow volumes bracket the field capacity calculated with Eqs. (1a,b), suggesting that the assumed regolith depths and porosities, or the combination of these variables represented by Eqs. (1a,b), may be reasonable.

Although the model underpredicts the seasonal rainfall threshold, it reproduces the decrease in the daily rainfall threshold with increasing seasonal accumulation (Fig. 8A). The decrease in the daily rainfall threshold with increasing seasonal accumulation in the early stages of the monsoon may be explained by an analysis of hillslopes that are well below field capacity. Because hillslopes at steep slope angles do not require much excess moisture (i.e., $M - F_c$) to fail, moisture in a thin regolith on a steep slope may abruptly reach a critical threshold during a day of intense rainfall early in the season (Fig. 9). Although subjected to the same rainfall input, a thicker regolith on the same slope will not attain the critical threshold until later in the monsoon season. Consequently, as the season progresses and the regolith moistures approach field capacity, the daily rainfall threshold decreases for the distribution of slopes and regolith thicknesses in the model.

The model (Fig. 8A) also replicates well the observation from the field data (Fig. 4) that not every rainfall value that falls within the landsliding field, defined by the seasonal accumulation and daily rainfall thresholds, triggers a landslide. The combined stochastic distributions of hillslope angles and regolith thicknesses set each hillslope along its own trajectory with the thresholds emerging as a landscape-scale feature.

The modeled distribution of failures within the daily-rainfall and seasonal-accumulation parameter space (Fig. 8A) suggests a relationship between these climatic variables and the geomorphic characteristics of the hillslopes that may fail (Fig. 10A,B). Overall, the regolith thickness controls the necessary accumulated rainfall before failure (Campbell, 1975), whereas slope steepness controls the daily rainfall necessary for failure (Fig. 10B). For example, given two hillslopes with similar storage capacities, the hillslope on a gentle slope will require a greater daily rainfall to

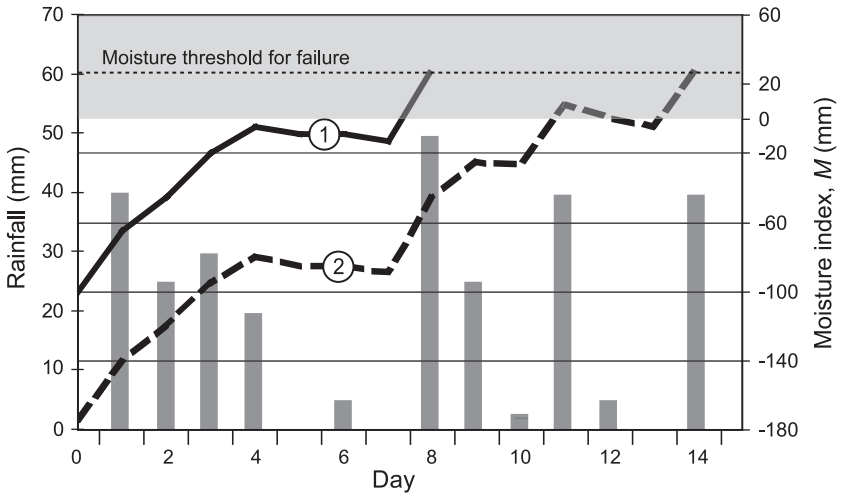

Fig. 9. Moisture paths of two steep hillslopes, with low but slightly different storage capacities, subjected to identical rainfall amounts. Both hillslopes are at identical slope angles so they both fail when they reach the identical moisture index (30 mm). Because Hillslope 1 has a lower storage capacity, the critical soil moisture is reached during a day of high rainfall intensity (Day 8), despite being significantly below field capacity on the previous day, and the hillslope fails. In contrast, Hillslope 2 is able to absorb the rainfall on Day 8 without reaching the critical soil moisture. Hillslope 2 fails later during a day of lower rainfall intensity (Day 14). This scenario, repeated over a distribution of slope angles and regolith depths, results in the observed and modeled decline in daily precipitation threshold as the seasonal accumulation increases. The shaded area represents soil moistures that lead to positive pore pressures.

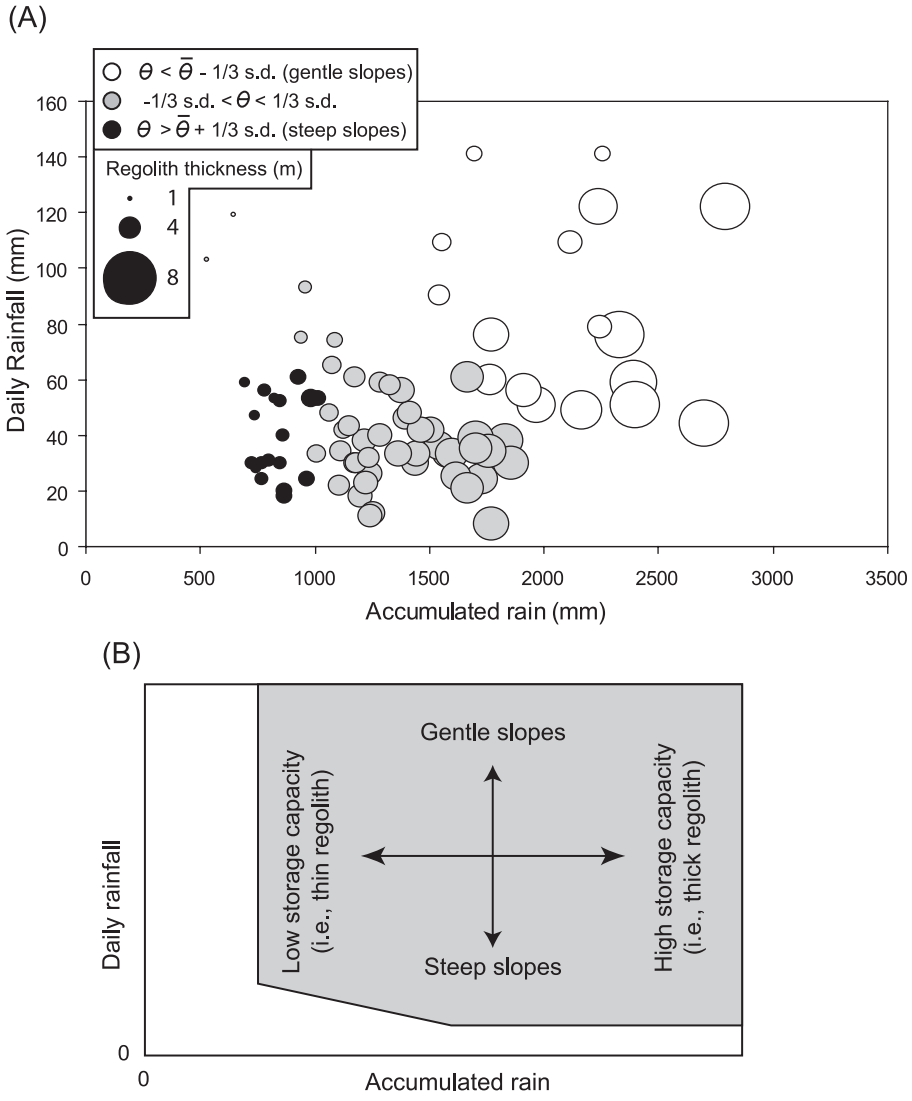

Fig. 10. (A) Hillslope characteristics of slopes that failed in the model. Hillslopes are divided into three categories according to deviation of slope angle from the mean ($\bar{\theta}$) and bubble widths are proportional to regolith thickness. Note that steep slopes with thick regolith are never stable according to the model and, therefore, are not represented. Additionally, because hillslopes are not resurrected once they fail in the model, the steep slopes are exhausted early in the season. (B) General relationships between rainfall and the characteristics of hillslopes that fail. Steeper slopes require lower positive pressures and, therefore, smaller amounts of daily rainfall to fail. Hillslopes with thicker regolith require greater amounts of antecedent rainfall to fail.

fail than a hillslope on a steeper slope because of the greater pore pressure required (Fig. 10A). Also, given two hillslopes at similar slope angles, the hillslope with lower storage capacity will fail earlier in the season than one with greater storage capacity (Fig. 10A). This relationship between rainfall amounts and landslide (i.e., regolith) thickness is supported by observations elsewhere. For example, in Puerto Rico, Larsen and Simon (1993) reported that short duration, high intensity storms triggered relatively shallow landslides; whereas the deepest landslides were triggered by long duration, low intensity storms. Similar observations were made by Wieczorek (1987) in California.

4. Conclusion

Rainfall data and daily sediment loads from a catchment in the Nepalese Himalayas are used to explore the effects of rainfall and hillslope characteristics on the initiation of landslides during the monsoon season. We found that two distinct rainfall amounts, a seasonal accumulation threshold and a daily rainfall threshold, must be exceeded before landslides are triggered. To investigate the controls on these thresholds, we present a slope stability model that is driven by daily rainfall and accounts for changes in regolith moisture. Results from the model show a similar pattern of rainfall thresholds to the field data. We conclude that slope angle controls the amount of daily rainfall necessary to destabilize a given hillslope and that the water storage capacity of the regolith determines the amount of seasonal rainfall needed to trigger a failure. Although the model does not duplicate all of the details of the landsliding record, it appears to define successfully the input parameters, both from the landscape and the climate, that control shallow slope failures in the Himalayas. More extensive field observations on a specific catchment might permit a more detailed "tuning" of the model to local conditions. As presented here, this model provides a coarse predictive tool for exploring interactions between monsoonal rainfall and hillslope stability, and it may underpin improved forecasting of imminent landslide hazards in the Himalayas.

Acknowledgements

A. Johnstone and A. Duvall provided invaluable assistance in the field. We thank T. Dunne and J. Garcia for discussions and R. Marston and an anonymous reviewer for comments on the manuscript. This research was supported by the NSF Continental Dynamics Program (EAR 9909647) and by NASA (NAGS-7781, -9039, -10520).

References

Anderson, M.G., Burt, T.P., 1978. The role of topography in controlling throughflow generation. Earth Surface Processes 3, 331–344.

Barros, A.P., Joshi, M., Putkonen, J., Burbank, D.W., 2000. A study of the 1999 monsoon rainfall in a mountainous region in central Nepal using TRMM products and rain gauge observations. Geophysical Research Letters 27, 3683–3686.

Benda, L.E., Dunne, T., 1997. Stochastic forcing of sediment supply to channel networks from landsliding and debris flow. Water Resources Research 33 (12), 2849–2863.

Beven, K., Germann, P., 1982. Macropores and water flow in soils. Water Resources Research 18 (50), 1311–1325.

Burbank, D.W., Blythe, A.E., Putkonen, J.K., Pratt-Situala, B.A., Gabet, E.J., Oskin, M.E., Barros, A.P., Ohja, T.P., 2003. Decoupling of erosion and climate in the Himalaya. Nature 426, 652–655.

Caine, N., 1980. The rainfall intensity-duration control of shallow landslides and debris flows. Geografiska Annaler 62A, 23–27.

Caine, N., Mool, P.K., 1982. Landslides in the Kolpu Khola drainage, Middle Mountains, Nepal. Mountain Research and Development 2 (2), 157–173.

Campbell, R.H., 1975. Soil Slips, Debris Flows, and Rainstorms in the Santa Monica Mountains and Vicinity, southern California. Professional Paper, vol. 851. USGS, Washington, DC. 50 pp.

Cannon, S.H., Ellen, S.D., 1985. Rainfall conditions for abundant debris avalanches. California Geology 38 (267), 267–272.

Chleborad, A.F., 2000. Preliminary Method for Anticipating the Occurrence of Rainfall-induced Landslides in Seattle, Washington. Open-File Report, vol. 00-469. USGS, Washington, DC. 30 pp.

Colchen, M., Le Fort, P., Pecher, A., 1986. Annapurna-Manaslu-Ganesh Himal. Centre National de la Recherche Scientifique, Paris, pp. 75–136.

Crozier, M.J., 1999. Prediction of rainfall-triggered landslides: a test of the antecdent water status model. Earth Surface Processes and Landforms 24, 825–833.

Dunne, T., Leopold, L.B., 1978. Water in environmental planning. W.H. Freeman and Co., New York. 818 pp.

Gabet, E.J., Dunne, T., 2003. A stochastic sediment supply model for a mediterranean landscape. Water Resources Research 39 (9), 1237 (10.1029/2003WRR002341).

Hovius, N., Stark, C.P., Hao-Tsu, C., Jiun-Chuan, L., 2000. Supply and removal of sediment in a landslide-dominated mountain belt: Central Range, Taiwan. Journal of Geology 108, 73–89.

Iverson, R.M., 2000. Landslide triggering by rain infiltration. Water Resources Research 37 (7), 1897–1910.

Keefer, D.K., Wilson, R.C., Mark, R.K., Brabb, E.E., Brown, W.M., Ellen, S.D., Harp, E.L., Wieczorek, G.F., Alger, C.S., Aitkin, R.S., 1987. Real-time landslide warning during heavy rainfall. Science 238 (4829), 921–925.

Lambert, L., Chitrakar, B.D., 1989. Variation of potential evapotranspiration with elevation in Nepal. Mountain Research and Development 9 (2), 145–152.

Larsen, M.C., Simon, A., 1993. Rainfall-threshold conditions for landslides in a humid-tropical system, Puerto Rico. Geografiska Annaler 75A, 13–23.

Leopold, L.B., Wolman, M.G., Miller, J.P., 1964. Fluvial Processes in Geomorphology. W.H. Freeman and Co., San Francisco. 522 pp.

Lloyd, C.R, Gash, J.H.C., Shuttleworth, W.J., de Marques, A.O., 1988. The measurement and modelling of rainfall interception by Amazonian rain forest. Agricultural and Forest Meteorology 43, 277–294.

Marston, R.A., Miller, M.M., Devtoka, L.P., 1998. Geoecology and mass movement in the Manaslu-Ganesh and Langtang-Jugal Himals, Nepal. Geomorphology 26 (1–3), 139–150.

Matthias, J., Weatherly, H., 2003. A hydroclimatic threshold for landslide initiation on the North Shore Mountains of Vancouver, British Columbia. Geomorphology 54 (3–4), 137–156.

Schenk, H.J., Jackson, R.B., 2002. The global biogeography of plant roots. Ecological Monographs 72 (3), 311–328.

Shroder Jr., J.F., 1998. Slope failure and denudation in the western Himalaya. Geomorphology 26 (1–3), 81–105.

Shroder Jr., J.F., Bishop, M.P., 1998. Mass movement in the Himalaya: new insights and research directions. Geomorphology 26 (1–3), 13–35.

Usman, S., Singh, S.P., Rawat, Y.S., 1999. Fine root productivity and turnover in two evergreen central Himalayan forests. Annals of Botany 84, 87–94.

Wieczorek, G.F., 1987. Effect of rainfall intensity and duration on debris flows in central Santa Cruz Mountains, California. In: Costa, J.E., Wieczorek, G.F. (Eds.), Reviews in Engineering Geology, vol. 7. Geological Society of America, Boulder, CO, pp. 93–104.